HHS Public Access

Author manuscript

Med Image Comput Comput Assist Interv. Author manuscript; available in PMC 2019 April 03.

Published in final edited form as:

Med Image Comput Comput Assist Interv. 2018 September ; 11072: 689–697. doi: 10.1007/978-3-030-00931-1_79.

Patch-based Mapping of Transentorhinal Cortex with a Distributed Atlas

Jin Kyu Gahm[1], **Yuchun Tang**[1,2], and **Yonggang Shi**[1]

[1]Laboratory of Neuro Imaging, USC Stevens Neuroimaging and Informatics Institute, Keck School of Medicine, University of Southern California, Los Angeles, USA

[2]Research Center for Sectional and Imaging Anatomy, Shandong University Cheeloo College of Medicine, Jinan, Shandong, China jkgahm@loni.usc.edu

Abstract

The significance of the transentorhinal (TE) cortex has been well known for the early diagnosis of Alzheimer's disease (AD). However, precise mapping of the TE cortex for the detection of local changes in the region was not well established mostly due to significant geometric variations around TE. In this paper, we propose a novel framework for automated patch generation of the TE cortex, patch-based mapping, and construction of an atlas with a distributed network. We locate the TE cortex and extract a small patch surrounding the TE cortex from a cortical surface using a coarse map by FreeSurfer. We apply a recently developed intrinsic surface mapping algorithm based on Riemannian metric optimization on surfaces (RMOS) in the Laplace-Beltrami embedding space to compute fine maps between the small patches. We also develop a distributed atlas of the TE cortex, formed by a shortest path tree whose nodes are atlas subjects, to reduce anatomical misalignments by mapping only between similar patches. In our experimental results, we construct the distributed atlas of the TE cortex using 50 subjects from the Human Connectome Project (HCP), and show that detailed correspondences within the distributed network are established. Using a large-scale dataset of 380 subjects from the Alzheimer's Disease Neuroimaging Initiative (ADNI), we demonstrate that our patch-based mapping with the distribute atlas outperforms the conventional centralized mapping (direct mapping to a single atlas) for detecting atrophy of the TE cortex in the early stage of AD.

1 Introduction

According to the Braak staging of Alzheimer's disease [1], the neurodegenerative process of AD begins in the transentorhinal (TE) cortex, and spreads to the hippocampus, the temporal and insular cortices, and eventually to the entire cortex. Therefore, the *in vivo* detection of localized changes in the TE cortex from MRI is critical for the early diagonosis of AD, so accurate mapping of the TE cortex is needed. Spherical registration-based mapping of entire cortical surfaces has been most widely used [2] but has a limitation with the accurate mapping of small and variable cortical structures such as the TE cortex (see Fig. 1). Therefore, a focused mapping of small patches including the target TE and neighboring structures and construction of a TE atlas on the patches have the potential of more precisely mapping this critical region. Recently, we have developed a novel approach of intrinsic surface mapping in the Laplace-Beltrami (LB) embedding space based on Riemannian

metric optimization on surfaces (RMOS) [3,4]. In our previous work, RMOS has been applied only to the genus-zero structures of the thalamus and striatum, but is applicable to general structures with various topology including patches whose Euler number is 1. In this work, we propose a novel framework for automatically generating the small patches from entire cortical surfaces using FreeSurfer's coarse maps, and producing fine maps between the small patches using RMOS.

One of the main challenges in studying the TE cortex and neighboring structures in the medial temporal lobe (MTL) is the existences of significant variations in the sulcal patterns. In particular, the continuous/discontinuous collateral sulcus (CS), and the no/shallow/deep rhinal sulcus (RS) were shown in different subjects from autopsy brains [5]. The continuous/discontinuous CS is also clearly observed on cortical surfaces from *in vivo* MRI as shown in Fig. 1. For a large-scale study of the TE cortex, therefore, mapping of the TE cortex from a single atlas with specific sulcal patterns to subjects with the various sulcal patterns, which we call a *centralized atlas*, is not appropriate. Instead, we construct an atlas network of multiple TE patches with various sulcal patterns whose connections are made only between similar patches, which we call a *distributed atlas*. Recently, such a distributed network (graph) of images was developed for image registration to reduce registration error by registering only similar images nearby in the graph [6].

Our distributed atlas of the TE cortex with RMOS maps for its connections is reusable and generally applicable to any study with different group/project subjects. In our experiments, we build the distributed atlas using a dataset of 50 subjects from the Human Connectome Project (HCP) [7]. Using a large-scale study dataset of 380 subjects from the Alzheimers Disease Neuroimaging Initiative (ADNI) [8], we demonstrate that our novel framework of automated patch generation and patch-based RMOS mapping with the distributed atlas achieves significantly improved sensitivity in the detection of TE atrophy in the early stage of AD, compared to RMOS and FreeSurfer mapping with the centralized atlas.

2 Methods

In this section, we describe the details of our novel framework for precise mapping of the TE cortex with a distributed atlas as well as present the theoretical backgrounds for patch-based RMOS.

Automated Patch Generation.

To extract small patches of the TE cortex from entire cortical surfaces, we first perform FreeSurfer reconstruction of T1-weighted MRI that generates surface representation and parcellation of the cortex [9, 10]. We randomly choose one subject as a reference, and manually delineate on the reference cortical surface a small but extensive patch region including the TE cortex and neighboring structures around the MTL to prevent the pattern of primary sulcus such as the CS near the TE cortex from being discontinued at the boundaries of the patch. More specifically, using the FreeSurfer's cortical parcellation results (*aparc +aseg*), we include the entire parahippocampal (PH) and entorhinal cortices (EC) with extension to the lateral side; the anterior parts of the fusiform and the inferior temporal cortex; and a half of the temporal pole adjacent to EC. Then we compute coarse maps of

cortical surfaces from other subjects to the reference using FreeSurfer (*mris register*) using the surfaces (*lh.white*) and features (*lh.sulc* and *lh.inflated.H*) in the FreeSurfer reconstruction results. Then using the FreeSurfer maps, we pull back the ROI labels from the reference surface onto the cortical surface (*lh.pial*) of each subject, smooth by mesh evolution and decimate the surfaces with the ROI labels to 25K vertices. We extract by the labels the patches with about 2K vertices from the cortical surfaces, and remove unconnected parts and holes ensuring that the final patches have the Euler number of 1. This process is fully automatic for a large-scale study with different subjects once we provide the reference cortical surface with the labels of the patch as a part of our atlas of the TE cortex.

RMOS Mapping of Patches.

After we extract the patches using FreeSurfer's coarse maps of large cortical surfaces, we compute fine maps between the small patches using RMOS [3,4]. Let $\mathscr{P}_i$ ($i = 1, 2$) denote the triangular mesh representation of two patches, and W_i denote their Riemannian metrics, *i.e.*, the edge weights. Using the Riemannian metrics, the LB embeddings of $\mathscr{P}_i$ can be computed as:

$$I^{\Phi_i}_{\mathscr{M}_i}(x) = \left(\frac{f^i_1(x)}{\sqrt{\lambda^i_1}}, \frac{f^i_2(x)}{\sqrt{\lambda^i_2}} \cdots, \frac{f^i_n(x)}{\sqrt{\lambda^i_n}}, \cdots \right) \ \forall x \in \mathscr{P}_i, \quad (1)$$

where λ^i_n and f^i_n are the n-th eigenvalue and eigenfunction of $\mathscr{P}_i$. Given L features ξ^j_1 and ξ^j_2 ($j = 1, \cdots, L$) defined on the patches, we compute the data term with the patch maps $u_1 : \mathscr{P}_1 \to \mathscr{P}_2$ and $u_2 : \mathscr{P}_2 \to \mathscr{P}_1$ as:

$$E_F(\mathscr{P}_1, \mathscr{P}_2) = \sum_{j=1}^{L} \left[\int_{\mathscr{P}_1} \left(\xi^j_1 - \xi^j_2 \circ u_1 \right)^2 d\mathscr{P}_1 + \int_{\mathscr{P}_2} \left(\xi^j_2 - \xi^j_1 \circ u_2 \right)^2 d\mathscr{P}_2 \right]. \quad (2)$$

We iteratively alternate the energy minimization of the data term E_F with a regularization term, and matching of the embeddings, *i.e.*, the eigenfunctions by updating the Riemannian metrics W_i in a gradient descent way. For the data term, in this work, we use three geometric features extracted from - FreeSurfer's sulcal depth, and curvature on the inflated surface; and the mean curvature (MC) computed from the normalized cortical surface to the average surface volume. Figure 2 illustrates RMOS mapping between two non-isometric patches (A, B) whose eigenfunctions, especially the 6th eigenfunctions (C, D), are largely different. With the optimized metrics plotted in Fig. 2 (E, F), the eigenfunctions become well matched (G, H). From the optimized LB embeddings, we compute the point-wise maps between the patches, and visualize the map from the source patch to the target patch by projecting the source patch onto the target patch (Fig. 2 (J)), and pulling back the MC from the target patch to the source patch (I), where the MC features of the target patch are well aligned to the source patch (A).

Distributed Atlas Construction.

Given an atlas dataset of N subjects, we construct a distributed atlas that is a tree-structured graph whose nodes are the N atlas subjects. Edges represent geometric dissimilarities of the patches between any pair of two nodes $\mathscr{P}_i$ and $\mathscr{P}_j$ with weights defined by the data term E_F in Eq. 3 using the initial nearest point map in the LB embedding space:

$$D_{i,j} = \exp\left\{E_F\left(\mathscr{P}_i, \mathscr{P}_j\right)/(\alpha\sigma)\right\} \quad (3)$$

where σ is the Gaussian kernel width set as the average data term, and α is the parameter that decides the tree height. We determine the root node, *i.e.*, the common space node, which is the shortest to all other nodes by the sum of the dissimilarity measures between their patches. Then we find the shortest path from the root node to every node that forms a tree-structured graph as the distributed atlas. We empirically adjust the parameter α that forms the tree of height > 1. The tree of height 1 is not desirable since direct mapping from the root to other nodes with significantly different sulcal patterns in the distributed atlas network may fail to establish anatomically correct correspondences. For each connection in the graph (total N-1 edges), we run RMOS mapping between similar patches of the edge nodes. In the RMOS maps, each point in one patch is discretized as a linear combination of vertex positions in the other patch. For any node of depth > 1, therefore, the composition of the maps along the path is done by combining the (point-wise) linear transformations and projecting the position of the final composite points onto the target patch.

TE Mapping with the Distributed Atlas.

For a large-scale study with different subjects, once the reference patch label, and the distributed atlas and its connection maps are provided, mapping of the TE cortex for the new subjects is fully automatic and straightforward by following the steps: 1) Run FreeSurfer reconstruction; 2) Compute coarse maps to the reference using FreeSurfer, and extract patches with the features by the maps; 3) Compute the dissimilarities of the patches between every subject and the atlas (every node); 4) Connect each subject to the shortest node in the distributed atlas; 5) Compute fine RMOS maps of the patches for the new connections, and composite maps along the path between each leaf (subject) and the root. The distributed atlas is generally applicable to any study so it is not required to rebuild it with new subjects.

3 Results

In this section, we present experimental results of our novel framework for precise mapping of the TE cortex with a distributed atals that signifcantly improved sensitivity in the early detection of TE atrophy by AD.

Generation of TE Patches.

We first demonstrate automated generation of patches for construction of the distributed atlas from 50 subjects of the Q1-Q3 release of HCP. Note that our experiments in this paper only focused on the left hemisphere. As shown in Fig. 3 (A), we delineated the ROI including TE on the reference cortical surface of a randomly chosen subject. The pullback

ROI of the reference to two other subjects by the FreeSurfer cortical maps are shown in Fig. 3 (B), and moderately well matched the actual anatomical ROI we defined on the reference cortical surface. We collected the sulcal depth and curvature maps on the cortical surfaces from the FreeSurfer reconstruction results, and computed the normalized MC of the original cortical surfaces. We decimated the cortical surfaces with the three feature maps to 25K, and extracted the patches and features as shown in Fig. 3 (C).

TE Cortex Delineation.

To evaluate the performance of patch-based mapping of the TE cortex in the distributed atlas, we delineated the TE cortex on each patch of the 50 HCP subjects. The TE cortex locates in the medial bank of the CS, and is the medial portion of the perirhinal cortex, which is bordered caudally by the PH cortex and ventrally and medially by the EC [11]. We used the FreeSurfer parcellation results to pinpoint the neighboring structures, and determined the TE boundaries by the CS and EC. Our delineation of the TE cortex for 3 subjects are shown in Fig. 4 (A) (colored in red).

Patch Mapping.

Figure 4 (A-C) demonstrates RMOS mapping of patches from an atlas to subjects. We set the RMOS parameters - the eigenorder 6, the regularization coefficient of 0.1, and the maximum 200 iterations. Direct mapping from the atlas to Subject b introduced large distortions in the projection of the atlas patch onto the Subject b patch, and the pullback TE labels of Subject b onto the atlas did not match well with the atlas TE labels as shown in Fig. 4 (B). Instead, mapping between more similar patches, determined from the dissimilarities measures between the patches in Eq. 3, from the atlas to Subject a, and from Subject a to b (Fig. 4 (A)), and composition of the two maps produced a high quality TE map with much less distortions as shown in Fig. 4 (C).

Distributed Atlas Construction.

We computed all the dissimilarities of the patches in Eq. 3 between every pair of the 50 subjects. We found the root node shortest to every other node from which we constructed the tree-structured distributed atlas of height 4 by setting the parameter $\alpha = 0.2$ in Eq. 3, as shown in Fig. 4 (D). We evaluated the quality of the TE maps in the distributed network between the 49 subjects and one root (atlas) using the dice coeffcient (DC), in comparison with direct maps from each subject to the atlas root by RMOS and FreeSurfer as shown in Fig. 4 (E). Obviously, FreeSurfer's surface mapping of the entire cortex produced poor performance. Both direct and distributed mapping of the small patches using RMOS achieved much better alignment of TE. However, the direct maps completely misaligned the TE regions for the two subjects (extreme outliers in the box plot). There was no misalignment for any subject by the distributed maps.

TE Atrophy by Early AD.

In the last experiment, we examined localized thickness changes of the TE cortex on patches during the development of AD using 380 subjects from ADNI 2 that consist of 105 normal control (NC), 132 early and 92 late mild cognitive impairment (EMCI, LMCI), and 51 AD.

Using the distributed atlas constructed from the HCP data, we extracted patches, established new connections to the distributed atlas, and computed their RMOS maps. We also computed RMOS patch maps and FreeSurfer cortical maps with the centralized atlas, *i.e.*, direct mapping to the root atlas. Using the three different maps, we pulled back the cortical thickness of each subject extracted from the FreeSurfer reconstruction results (and normalized by total intracranial volume) to the root atlas, and applied vertex-wise t-test of the pullback thickness between the different groups. Figure 5 shows the p-value maps on the root atlas patch especially for thickness changes between NC vs. early AD (EMCI, LMCI). Clearly, our mapping approach with the distributed atlas found more regions of significant thickness change within the TE cortex between NC and other groups, particularly detected about 20% of the TE cortex at the posterior parts significant in atrophy in the very early stage of AD (EMCI).

4 Conclusion

In this paper, we developed a novel framework for automated patch generation and patch-based mapping of the TE cortex with a distributed atlas. The patch-based approach achieved higher accuracy of TE mapping than FreeSurfer, and mapping thorough the distributed atlas produced better anatomical matches than the centralized atlas mapping. The distributed atlas built with the HCP data worked well for the different ADNI data, and our novel framework of TE mapping achieved higher sensitivity in the early detection of AD. For future work, we will complete the experiments of TE atrophy for both hemispheres, and apply our distributed atlas approach for mapping of the subcortical structures or other cortical regions with a large amount of geometric variations.

Acknowledgments

This work was in part supported by the National Institute of Health (NIH) under Grant R01EB022744, P41EB015922, U01EY025864, U01AG051218, P50AG05142.

References

1. Braak H, Braak E: Neuropathological stageing of Alzheimer-related changes. Acta neuropathologica 82(4) (1991) 239–259 [PubMed: 1759558]
2. Fischl B, Sereno MI, Dale AM: Cortical surface-based analysis II: Inflation, flattening, and a surface-based coordinate system. NeuroImage 9(2) (1999) 195–207 [PubMed: 9931269]
3. Gahm JK, Shi Y: Riemannian metric optimization for connectivity-driven surface mapping. In: Proc. Med. Image Comput. Comput. Assist. Interv, Part I (2016) 228–236
4. Gahm JK, Shi Y: Holistic mapping of striatum surfaces in the Laplace-Beltrami embedding space. In: Proc. Med. Image Comput. Comput. Assist. Interv, Part I. Volume Part I (2017) 21–30
5. Ding SL, Van Hoesen GW: Borders, extent, and topography of human perirhinal cortex as revealed using multiple modern neuroanatomical and pathological markers. Human brain mapping 31(9) (2010) 1359–1379 [PubMed: 20082329]
6. Ying S, Wu G, Wang Q, Shen D: Hierarchical unbiased graph shrinkage (HUGS): a novel groupwise registration for large data set. NeuroImage 84 (2014) 626–638 [PubMed: 24055505]
7. Essen DCV, Smith SM, Barch DM, Behrens TE, Yacoub E, Ugurbil K: The WUMinn human connectome project: An overview. NeuroImage 80 (2013) 62–79 [PubMed: 23684880]
8. Mueller S, Weiner M, Thal L, Petersen RC, Jack C, Jagust W, Trojanowski JQ, Toga AW, Beckett L: The Alzheimer's disease neuroimaging initiative. Clin. North Am 15 (2005) 869–877 xi–xii

9. Dale AM, Fischl B, Sereno MI: Cortical surface-based analysis I: segmentation and surface reconstruction. NeuroImage 9 (1999) 179–194 [PubMed: 9931268]

10. Fischl B, van der Kouwe A, Destrieux C, Halgren E, Sagonne F, Salat DH, Busa E, Seidman LJ, Goldstein J, Kennedy D, Caviness V, Makris N, Rosen B, Dale AM: Automatically parcellating the human cerebral cortex. Cerebral Cortex 14(1) (2004) 11–22 [PubMed: 14654453]

11. Taylor KI, Probst A: Anatomic localization of the transentorhinal region of the perirhinal cortex. Neurobiology of aging 29(10) (2008) 1591–1596 [PubMed: 17478012]

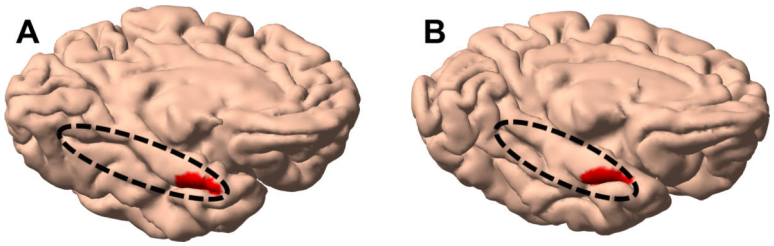

Fig. 1.

(A) Continuous and (B) discontinuous collateral sulcus, highlighted by the dashed ellipsoids, on left cortical surfaces reconstructed from *in vivo* T1-weighted MRI. The transentorhinal (TE) cortex is also shown in red color.

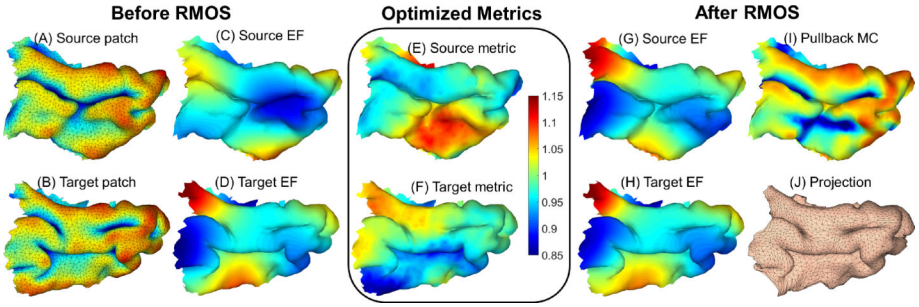

Fig. 2.

Illustration of RMOS mapping between (A) source and (B) target patches colored with their mean curvature (MC). (C, D) The 6th eigenfunctions (EFs) of the source and target patches before RMOS; and (G, H) the EFs after RMOS, with (E, F) the optimized Riemannian metrics. (I, J) The pullback of MC from the source to the target patch, and projection of the source onto the target patch by the RMOS map.

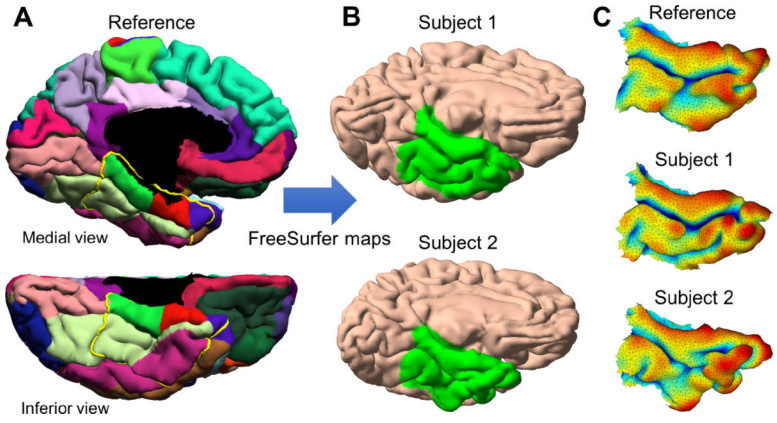

Fig. 3.

Automated patch generation of the left TE cortex with the neighboring structures. (A) Delineation of ROI (yellow curve) around the medial temporal cortex on a reference cortical surface guided by the FreeSurfer parcellation results. (B) Pullback labels (green) of the reference ROI onto subject's cortical surfaces by the FreeSurfer's cortical maps. (C) Extracted patches by the labels from the cortical surfaces, and colored with their mean curvature that ranges $[-0.4, 0.4]$ mm^{-1}.

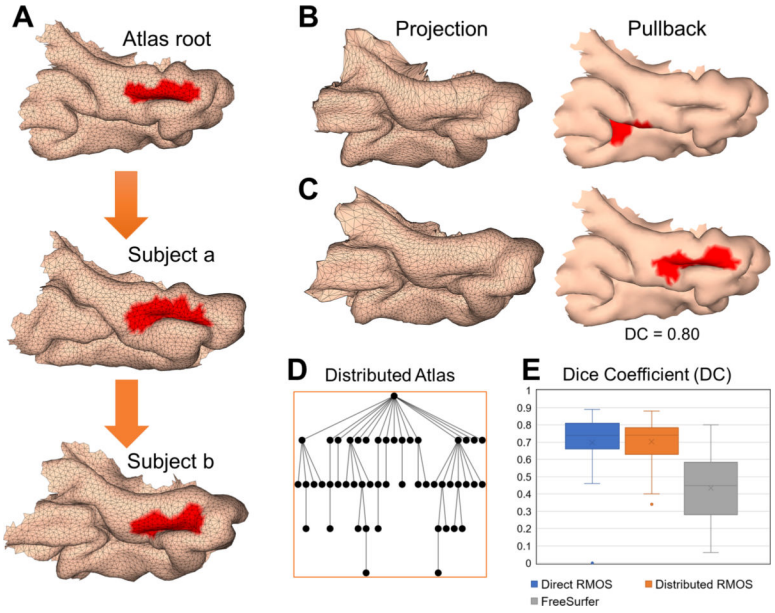

Fig. 4.

Patch-based mapping of the TE cortex, and distributed atlas construction. (A) Demonstration of RMOS mapping of patches from the atlas to Subject b through Subject a where TE were manually delineated (with red color). (B) Projection of the atlas patch onto Subject b patch, and pullback TE labels of Subject b onto the atlas patch by direct mapping from the atlas to Subject b; (C) by composition of the maps between the atlas and Subject a, and between Subject a and b. (D) Tree-structured distributed atlas constructed using an atlas dataset of 50 subjects from the HCP. (E) Box plots of overlap measures between the atlas root and pullback TE labels of other 49 atlas subjects by the direct, distributed RMOS maps, and direct FreeSurfer cortical maps.

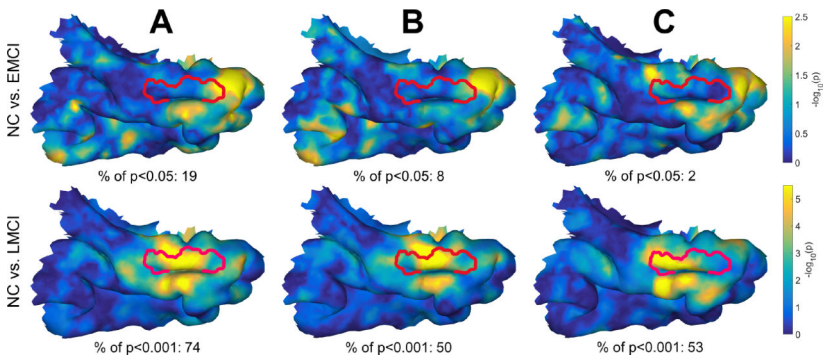

Fig. 5.

Log-scale *p*-value maps of thickness on the atlas root patch for the 105 normal control (NC) vs. 132 early mild cognitive impairment (EMCI) subjects, and the 105 NC vs. 92 late MCI (LMCI) subjects (A) using the distributed atlas and (B) the centralized atlas with RMOS, and (C) the centralized atlas with the FreeSurfer cortical maps. The boundary of the TE cortex we delineated on the atlas root patch is drawn by a red curve. The percentage of points in the TE cortex at which the *p*-value is less than 0.05 or 0.001 is shown below each *p*-value map.